

Landslides (2018) 15:581–592
 DOI 10.1007/s10346-018-0945-9
 Received: 12 February 2017
 Accepted: 4 January 2018
 Published online: 11 January 2018
 © Springer-Verlag GmbH Germany,
 part of Springer Nature 2018

Yuming Zhang · Xinli Hu · Dwayne D. Tannant · Guangcheng Zhang · Fulin Tan

Field monitoring and deformation characteristics of a landslide with piles in the Three Gorges Reservoir area

Abstract Landslides often occur within the reservoir area behind dams. In China, a common strategy for stabilizing these landslides is to install large piles through the landslide and into the stable ground below. The piles interact with the landslide and constitute a landslide-stabilizing pile system. The deformation of this system under the reservoir operation is more complicated than the deformation of the landslide itself. Understanding the behaviour of this system is very important to the long-term safety of landslides stabilized with piles in reservoirs. The Majiagou landslide, which was selected as a case study, was triggered by the first impoundment of the reservoir behind the Three Gorges dam. A row of anti-slide piles was installed in the landslide in 2007, but monitoring results found these were ineffective at stabilizing the landslide. Subsequently, in 2011, two longer test piles and an integrated monitoring system were installed in the landslide to better understand the failure mode of the landslide and to measure the deformation characteristics of the landslide-stabilizing pile system. Monitoring results show that the Majiagou landslide is a translational landslide with three slip surfaces. The test piles provided local resistance and partially slowed down the sliding mass behind the piles, and the landslide deformation response to external factors decreased for a time. However, after 2 years, the deformation of the landslide-stabilizing pile system reverted to seasonal stepwise cumulative displacements influenced by cycles of reservoir drawdown and rainfall. The monitoring results provide fundamental data for evaluating the long-term performance of anti-slide piles and for assessing long-term stability of the stabilized landslide under the reservoir operation.

Keywords Landslide-stabilizing pile system · Deformation characteristics · Field monitoring · Three Gorges Reservoir area

Introduction

The Three Gorges Reservoir in China is long and narrow and has approximately 2000 km of shoreline. The creation of the reservoir in 2003 initiated many new landslides. For example, the Qianjiangping landslide in Zigui County was caused by water level fluctuations and heavy rainfall (Cojean and Cai 2011). There are more than 5300 landslides in the reservoir area (Yi et al. 2011). Of these, 725 landslides have been stabilized with anti-sliding structures according to official statistics. Typically, a single row of large anti-slide piles is installed through the landslide and into the stable ground below to help stabilize the landslide. While anti-slide piles have been widely used around the world, including in the Three Gorges Reservoir area (Chen and Martin 2002; Zhou et al. 2014), questions remain about how these landslide-stabilizing pile systems function and deform under reservoir operations. Seeking answers to

these questions is fundamental to evaluating the long-term performance of anti-slide piles and to assessing long-term stability of the stabilized landslides.

The evolution of a landslide is a complicated process, controlled not only by basic geological, geomorphic, and hydrogeological properties but also by external factors. For reservoir landslides, the evolution process is more complicated due to the effect of varying reservoir water levels. In the Three Gorges Reservoir area, many landslides occur on weak sedimentary rock layers that can be easily softened by water. For example, the Majiagou landslide developed on the purple-red mudstone of the Jurassic Suining Formation strata and the Huangtupo landslide developed on the middle Triassic Badong Formation strata. Studies have shown that rainfall and water level fluctuations are the two dominant factors influencing the deformation of landslides in the Three Gorges Reservoir area (Hu et al. 2013; He et al. 2008; Wang et al. 2016, 2008; Xia et al. 2013). At present, numerical simulation methods (Lane and Griffiths 2000; Jian et al. 2009; Paronuzzi et al. 2013; Jiao et al. 2014; Jiang et al. 2016, Jiang and Zhou 2017) and physical model tests (Jia et al. 2009; Yan et al. 2010; Zhu et al. 2014) are widely used to study the stability and deformation of landslides affected by rainfall, water level fluctuations, and other conditions. In situ monitoring is another effective and practical way to reveal the landslide deformation. Moreover, monitoring can be used to verify the results of numerical and physical models. Through field monitoring, researchers (Wang et al. 2016, 2008; Yin et al. 2010; Massey et al. 2013; Hu et al. 2013; Palis et al. 2017; Ma et al. 2017) have studied reservoir landslide movements and their relationship with influencing factors. Analyzing the results from the field monitoring data is more reliable and accurate than results from modeling (physical or numerical). However, field monitoring is expensive and requires lengthy periods of time to gather data for different climate and reservoir level conditions.

For landslide-stabilizing pile systems, research has focused on two aspects: (1) the interaction mechanisms between the piles and the sliding mass, considering the pile spacing, pile embedment length, and the rock mass structure of the embedded layer (Kourkoulis et al. 2011; Guo 2015; Li et al. 2016; Sharafi and Sojoudi 2016) and (2) the evaluation of the effectiveness of anti-slide piles under heavy rainfall and reservoir water level fluctuation (Frank and Pouget 2008; Smethurst and Powrie 2007; Wei et al. 2009).

This paper presents an extension of previous studies of the Majiagou landslide in the Three Gorges Reservoir area and presents monitoring results from two instrumented test piles. Based on field monitoring information, the landslide failure mode was determined, and the deformation characteristics of the landslide-stabilizing pile system were analyzed. This research provides

insight into the long-term stability of landslides stabilized with piles under reservoir operation.

General settings of Majiagou landslide

Geological setting

The Majiagou landslide is situated on the left bank of the Zhaxi River, a tributary river of the Yangtze River in Zigui County, Hubei Province (Fig. 1a, b). The Majiagou landslide was initiated when the reservoir behind the Three Gorges dam was first impounded in 2003. In plain view, the Majiagou landslide has an approximately rectangular shape (Fig. 1c) with a length of 537 m and an average width of about 180 m. The slope surface consists of alternatively gentle and comparatively steep landforms, with an average slope of 15°. The sliding direction is 291°, approximately perpendicular to the Zhaxi River.

Field investigations indicated that main geologic units of the Majiagou landslide are surficial deposits and sedimentary bedrock (Figs. 2 and 5). Exploratory trenching showed that the surficial deposits are loose gravel soils with a high permeability

(6.4×10^{-4} to 5.0×10^{-3} m/s) (Fig. 3a). The bedrock is weathered interbedded gray sandstone and purple-red mudstone of the Jurassic Suning Formation with a low permeability (1.3×10^{-7} to 6.0×10^{-6} m/s) (Fig. 3b). The bedrock dips 12° to 30° toward 275°, which is roughly the same as the landslide sliding direction. The purple-red mudstone can be easily softened by water and has low strength. The average annual rainfall is approximately 1000 mm. The reservoir water level fluctuates between an elevation of 145 and 175 m each year. The groundwater level changes as the reservoir water level fluctuates (Figs. 5 and 11).

Anti-slide piles and test piles

In 2007, 17 anti-slide piles (18 to 22 m length) were installed at an elevation of 200 m on the landslide surface to reduce movements. The sliding zone was determined from geological drilling (25 m length) and shaft excavation (15 m depth) in 2005 to be located at the interface between the surficial deposits and the bedrock at a depth of approximately 12 m. The embedded length of each pile into the bedrock is 8 to 10 m.

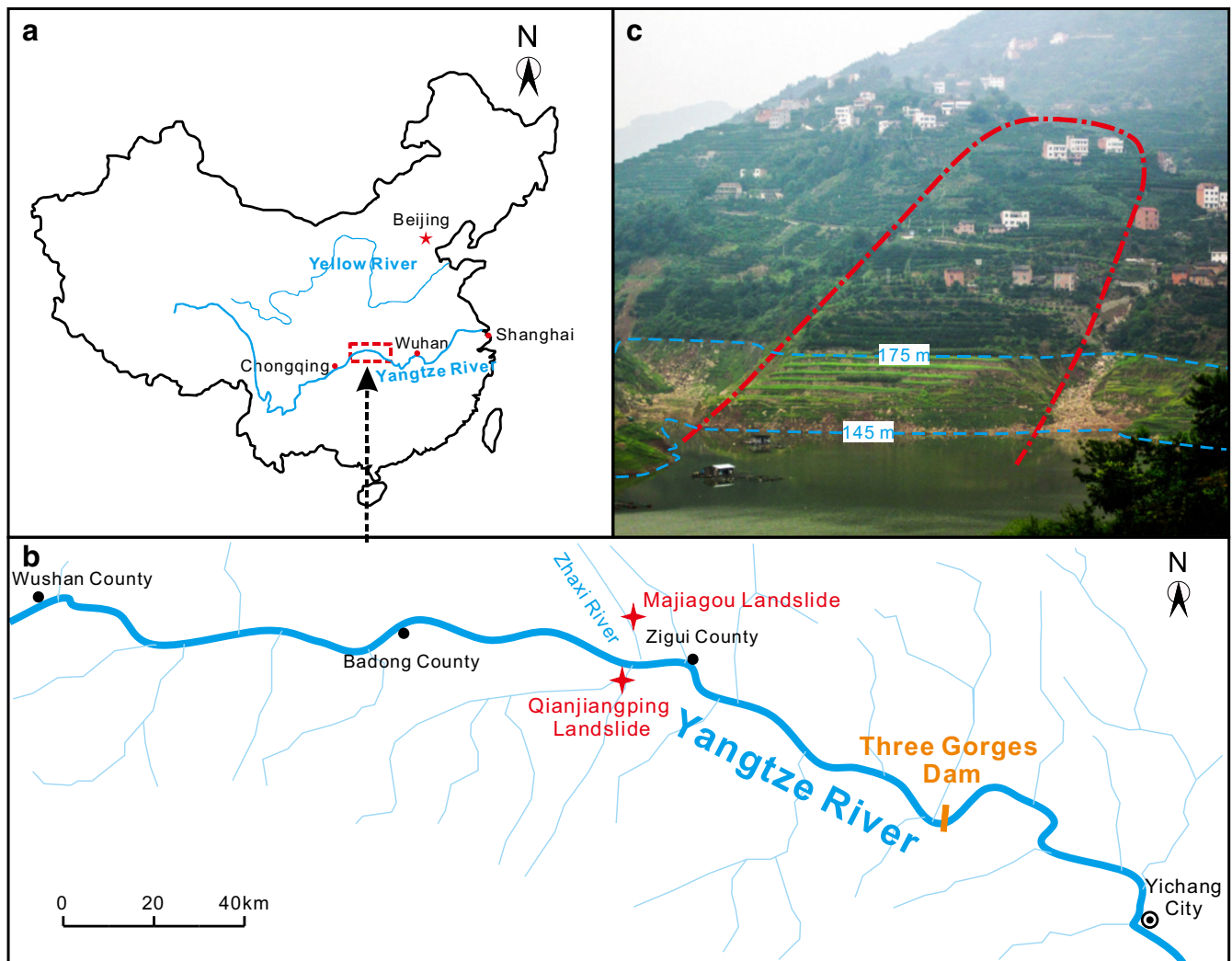


Fig. 1 Majiagou landslide in the Three Gorges Reservoir area

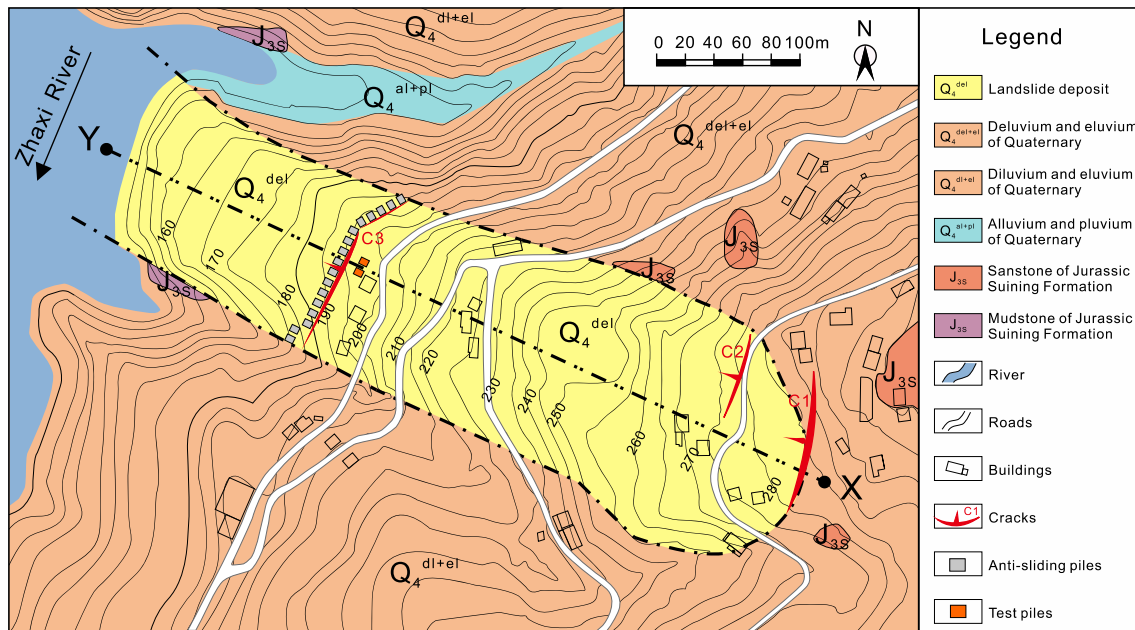


Fig. 2 Geological map of Majiagou landslide

Two stabilizing test piles (40 m length) were constructed in 2011 and are located 5.8 m upslope from the previously installed anti-slide piles. When pilot holes were drilled for the two test piles, a second slip surface at a depth of approximately 19 m below the surface was discovered. This surface was located in weak layers within the purple-red mudstone layer. The nature of this slip surface is discussed later in this paper.

Cracks

Three cracks were found on the landslide surface. Crack C1 (Fig. 4a) was found in 2003 at the top of the landslide. Crack C2 (Fig. 4b) was found in 2010, within a concrete paved road at an elevation of 274 m. The strikes of these two cracks are almost perpendicular to the sliding direction of the landslide. Crack C3 (Fig. 4c, d) was first found in 2009 and formed a gap between the piles and material upslope of the piles (Figs. 2 and 5). It enlarged gradually in response to the reservoir water level fluctuations and rainfall. The location and extension of this crack indicate that the

17 anti-slide piles are sliding together with the lower part of the landslide.

Monitoring system

An integrated monitoring system was designed and installed during the test pile construction. The monitoring system consists of surface displacement monitoring stations, inclinometers in boreholes, water level gauges, and strain gauges mounted to the test piles (Fig. 6).

Surface displacement monitoring stations

In 2007, five GPS monitoring stations (G01 to G05) were installed on the landslide surface (Figs. 5 and 6). In 2008, two additional stations (G12 and G13) were installed at the top of two piles to monitor pile displacements (Fig. 6). The monitoring data are available from March 2007 to November 2009.

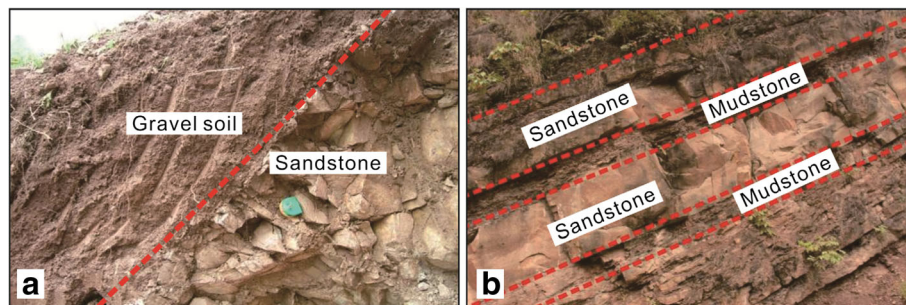


Fig. 3 Gravel and sandstone exposed by an exploratory trench (a) and interbedded sandstone and mudstone bedrock (b)

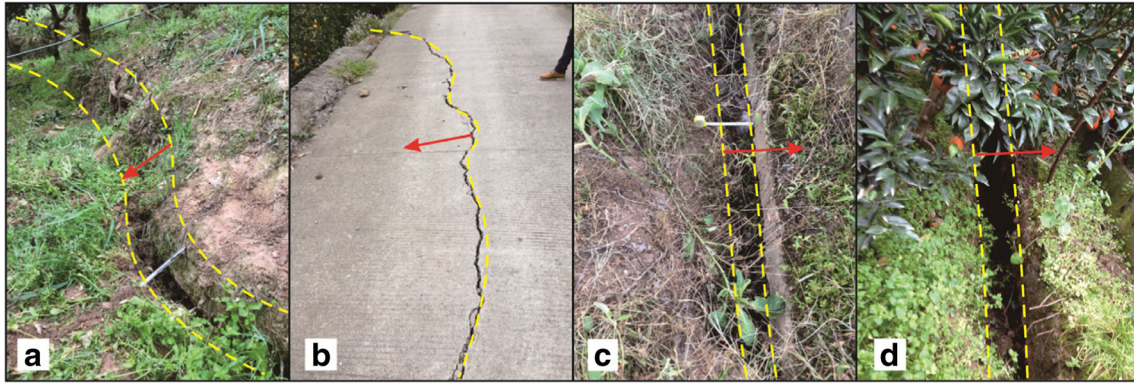


Fig. 4 Landslide cracks. a Crack C1 (2009). b Crack C2 (2013). c Crack C3 (2009). d Crack C3 (2013)

In 2012, three GPS monitoring stations, Ho1, Ho2, and Ho4, were installed to replace stations Go1, Go2, and Go4, respectively, and displacement monitoring began in October 2012.

Borehole inclinometer and water level gauges

Inclinometers and water level gauges were installed in a series of boreholes (Figs. 5 and 6). Inclinometers JC1 (40 m depth) and JC8 (43 m depth) are located at an elevation of 180 m and 225 m, respectively. Six additional inclinometers are located around the test piles, at depths of 38 to 40 m. Three water level gauges were installed at the bottom of inclinometers JC1, JC3, and JC8. In addition, three inclinometers OFS1 (40 m depth), OFS2 (28 m depth), and OFS3 (14 m depth) were installed at an elevation of 170, 248, and 274, respectively, by Nanjing University (Sun 2015).

Strain-gauged test piles

In each test pile, 26 vibrating wire strain gauges were installed to measure the longitudinal pile strain. These were installed as 13 pairs with a vertical spacing of 3 m. The gauges for each pair were embedded on the front and back surface of the test pile; thus, they were separated by the 2-m pile thickness (Fig. 6).

Monitoring results

Surface deformations

The movement of the surface monitoring stations and the rainfall, reservoir water level, and landslide velocity are presented in Fig. 7. The monitoring results are presented for two time periods: (a) after the main row of anti-slide piles were installed (February 2007 to November 2009) and (b) after the test piles were installed (October 2012 to February 2016). The reservoir water levels and rainfall data were obtained from official databases.

Surface deformation before test piles were installed

The cumulative displacement curve in Fig. 7a shows that the landslide movement increased continuously with time, and the row of piles was ineffective. During the monitoring period between 2007 and 2009, GPS monitoring station Go1 recorded the largest average annual deformation at approximately 183 mm/year. Each year, the displacement of Go1 shifts cyclically between low (0.1 to 0.5 mm/day) and high rates (0.5 to 2.25 mm/day) of movement in response to the reservoir water level fluctuation and rainfall. Consequently, the cumulative displacements curves are stepwise. The acceleration period

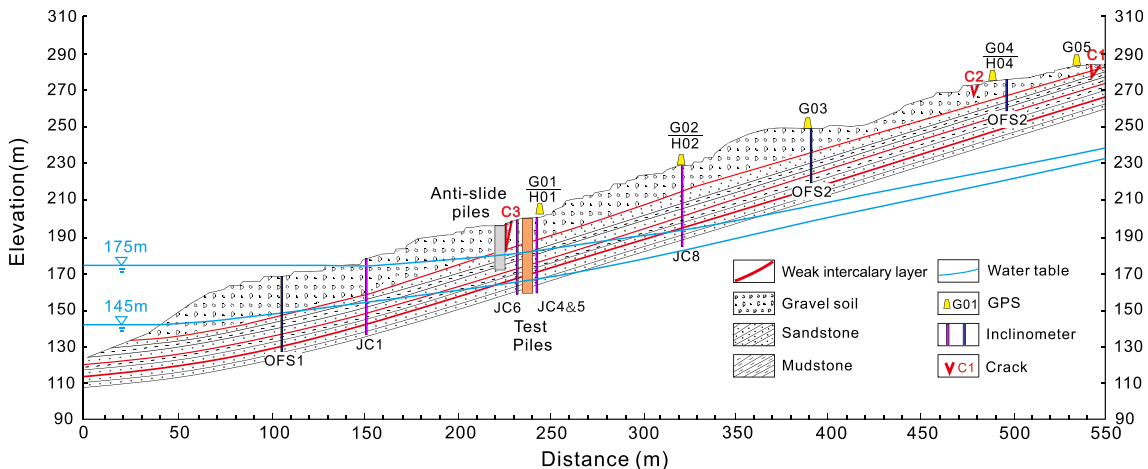


Fig. 5 Vertical profile of Majiagou landslide

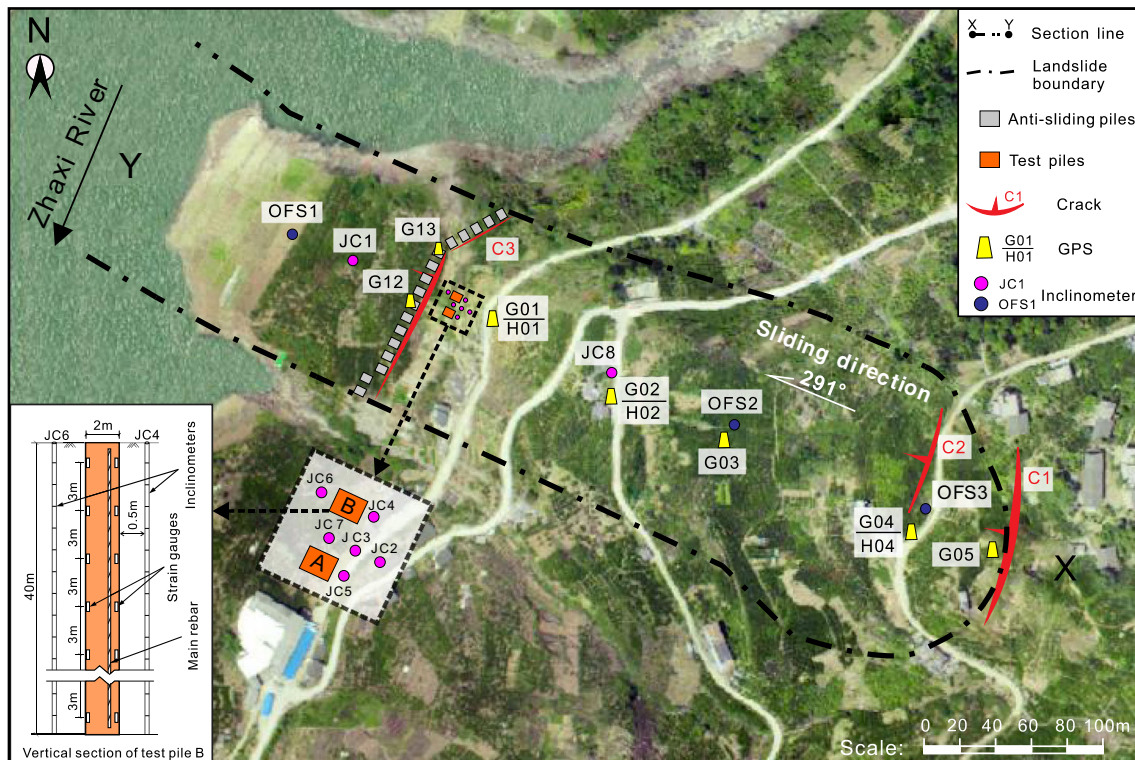


Fig. 6 Plan view of Majiagou landslide piles and monitoring system and vertical section of test pile B with monitoring sensors

almost coincides with the rainy season but lags about 2 months behind the reservoir water level decrease.

The magnitude of the landslide displacements decreased from the lower monitoring stations to the upper stations. The two GPS monitoring stations mounted on the anti-slide piles (G12 and G13) moved faster than other GPS stations on the landslide surface, which indicates that these piles were moving forward together with the lower portion of the landslide.

Surface deformation after test piles were installed

From Fig. 7b, the cumulative displacement curves of the three GPS stations (H01, H02, and H03) increased linearly from October 2012 to April 2014 after the test piles were installed. The velocity of the ground upslope of the test piles remained low (about 0.10 to 0.25 mm/day) with only a small fluctuation associated with reservoir water level drawdown and rainfall. This is due to the combined effect of resistance provided by the test piles and the lower rainfall in 2013. Over time, this stabilizing effect was gradually lost. From April 2014 to February 2015, the displacements rose abruptly twice with two periods of relatively high landslide velocities. The first peak with a velocity of 0.40 mm/day occurred in May 2014 and was caused by the combined effects of reservoir water level drawdown and rainfall. The second peak with a velocity of 0.53 mm/day occurred in September 2014 and was triggered by heavy rainfall that lasted for several weeks.

From February 2015 to February 2016, the deformation response of the ground upslope of the piles reverted to conditions

that existed before the test piles were installed. The time-series cumulative displacement curves began to show a stepwise pattern again.

Inclinometer deformations

Inclinometer data in Fig. 8 shows the presence of three sliding surfaces labeled S1, S2, and S3. Sliding surface S1 is located at the boundary between the superficial deposits and the bedrock, and this surface experienced small deformations. The sliding surface S2 occurs at a weak layer in the bedrock. It was exposed in the pile shafts and was detected by the inclinometers around the test piles at a depth of 19~20 m. It is 31.5 m deep in JC1 and merges with sliding surface S1 at JC8. The sliding surface S3 occurs in a layer of soft fractured purple-red mudstone at a depth of 27~29 m. Sliding surface S3 can also be detected at a 36-m depth in JC1 and a 36.5-m depth in JC8, where the two inclinometer casings broke in August 2014.

The Majiagou landslide is currently sliding along slip surfaces S2 and S3, with the largest shear displacements occurring along S3. The inclinometers around the test piles are still working and their displacement curves show a “V-shape” rather than a “P-shape” of JC1 and JC8, because the shear resistance provided by these piles has locally limited the displacements. In addition, the deformation of JC6 downslope of pile B is larger than of JC4 located upslope of the pile, which shows that the lower portion of the landslide below the piles is moving faster.

Time-series plots of displacements of the inclinometer tops are shown in Fig. 10. Inclinometer JC1 shows that the lower portion of

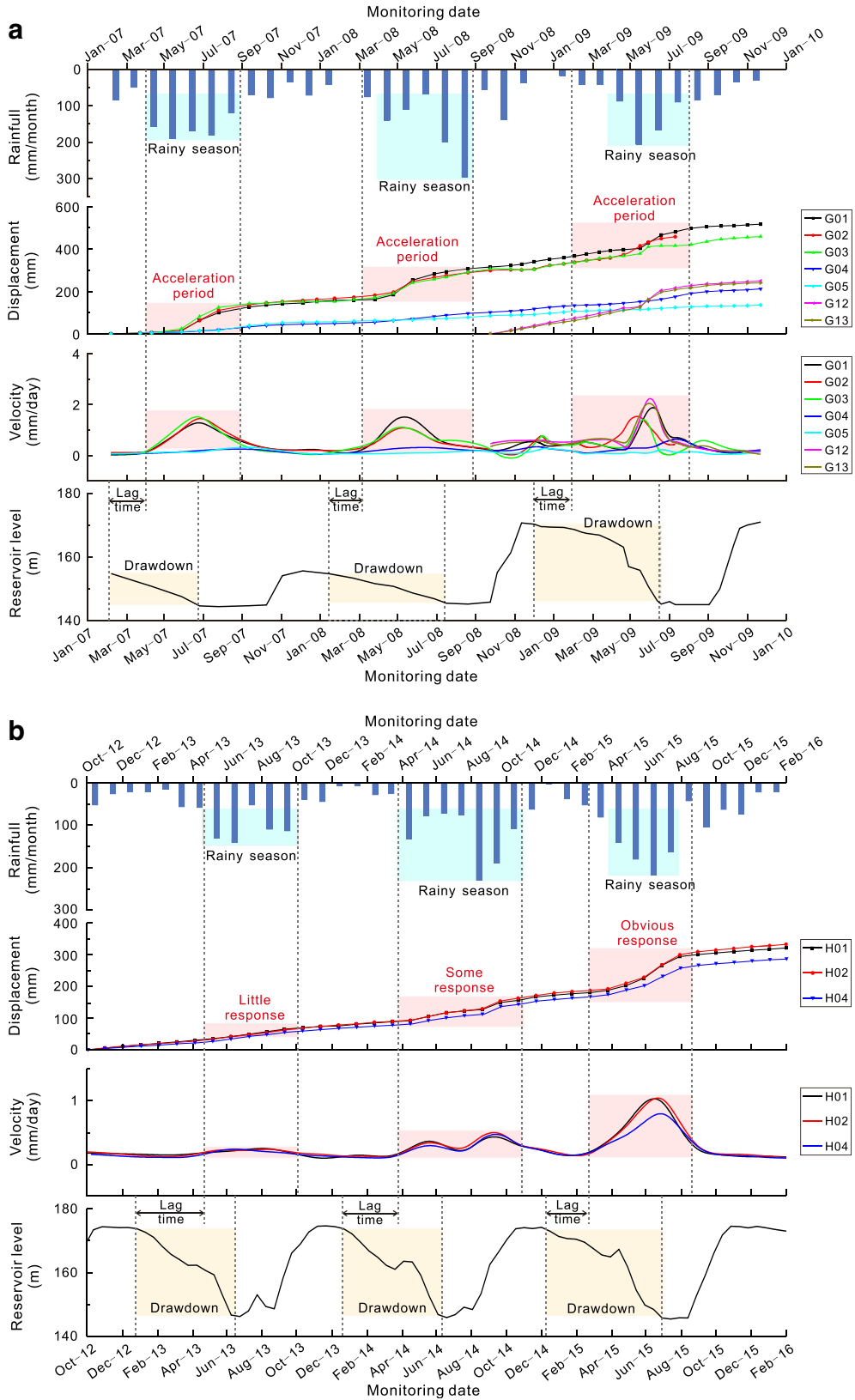


Fig. 7 Time-series of rainfall, water level, landslide displacement, and velocity a before test piles installed. b After test piles installed

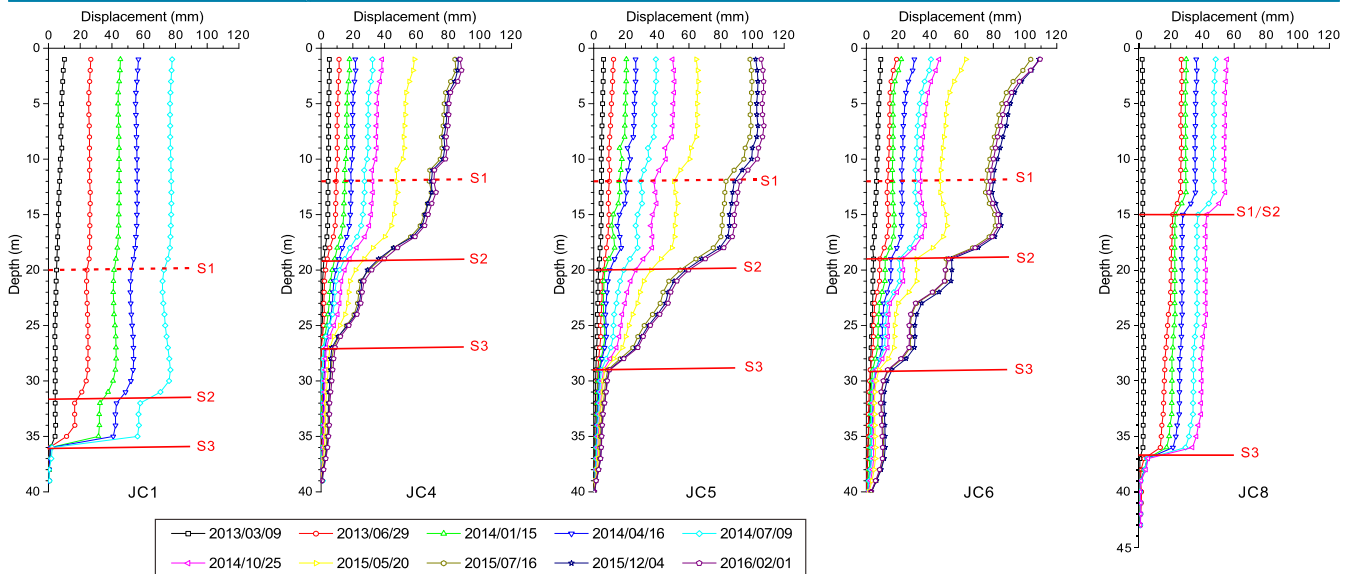


Fig. 8 Monitoring results from inclinometers

the landslide was the fastest moving, and the movement was affected by changes in the reservoir and rainfall. The time-series plots of other inclinometers around piles or behind piles are similar to the GPS monitoring results (Fig. 7b), but there is a cumulative difference of 203.78 mm between them. The possible reasons are given in the “Discussion” section at the end of this article.

Test piles strains and deflections

Figure 9a, b shows the measured strain distributions versus depth at the downslope and upslope sides of the two test piles. The strain distributions along the two piles are similar. The measured longitudinal strains can be converted into pile deflections using the theoretical equations below. Equation (1) (Lirer 2012) is based on standard engineering beam theory. Equation (2) is the relationship between the curvature of a plane curve and the derivative of the plane curvilinear equation:

$$\frac{1}{\rho} = \frac{M}{EI} = \frac{\varepsilon_{up} - \varepsilon_{dn}}{a} \tag{1}$$

$$\frac{1}{\rho} = \pm \frac{w''}{(1 + w'^2)^{3/2}} \tag{2}$$

where $1/\rho$ is the curvature of a pile, M is the bending moment, EI is the flexural rigidity of a pile, ε_{dn} and ε_{up} are the longitudinal strain at the downslope and the upslope sides of the pile, a is the distance between two gauges, and w is the lateral deflection of a pile.

In Eq. (2), w' can be ignored because it is much less than 1. Thus, the deflection w can be computed as follows:

$$w'' = \frac{\varepsilon_{up} - \varepsilon_{dn}}{a} \tag{3}$$

$$w = \int dz \int \frac{\varepsilon_{up} - \varepsilon_{dn}}{a} dz + C_1 z + C_2 \tag{4}$$

where z is the height of a strain gauge from the bottom of a pile ($z=0$ at the pile bottom and $z=40$ m at the pile top). The deflection and the curvature of a pile at the bottom are both zero, and this means that $w=0$ and $1/\rho=0$ when $z=0$. With this boundary condition, Eq. (5) can be used to calculate the deflection of a pile using the measured longitudinal strains:

$$w = \int dz \int \frac{\varepsilon_{up} - \varepsilon_{dn}}{a} dz \tag{5}$$

The calculated flexural deflections of the piles are shown in Fig. 9c, d. The test piles were bent downslope by the landslide mass moving along sliding surface S3. There is essentially no pile deflection below a depth of 29 m (pile A) and 27 m (pile B). The piles experienced their greatest bending over a depth of approximately 22 to 28 m. The upper 10 to 15 m of the piles incurred rigid body deflection associated with the bending motions at greater depths. The deflection displacement of the top of pile A is 133 mm while that of pile B is 102 mm as of February 2016. The larger deflection of pile A is consistent with the measurements taken from inclinometers JC4 and JC5. Furthermore, the depth of largest curvature is near the slip surface S3.

The time-series of the deflection at the pile tops are plotted in Fig. 10b. These plots display trends that are similar to the inclinometer results (Fig. 10a) and indicate that the test pile deflections are compatible with the differential movement along the three slip surfaces.

Groundwater level

The groundwater level changes with reservoir water level (Fig. 11). Rainfall has little effect on the fluctuation of groundwater level because the rainfall is less than 300 mm/month.

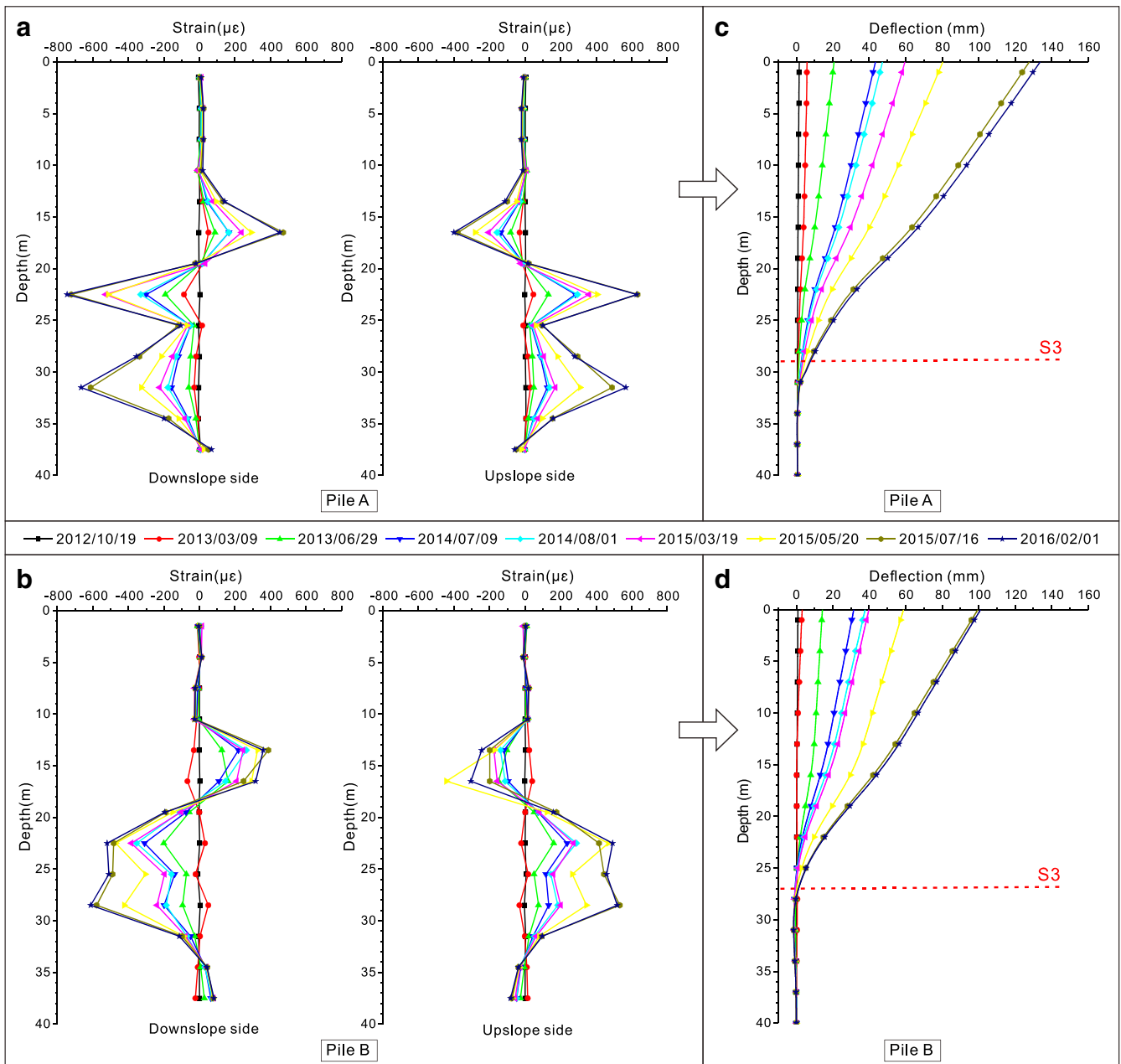


Fig. 9 Measured strains and deflection of test piles

Due to the high permeability of the surficial deposits and the short distance between piezometer JC1 and the reservoir, the groundwater level at JC1 fluctuated synchronously with the reservoir level. However, the decreases of the groundwater levels at JC3 and JC8 generally lagged about 2 to 3 months behind the reservoir water level decreases because of the low permeability of the bedrock. When the reservoir water level decreases, the lag in the drop in the groundwater level in the bedrock increases the hydraulic gradient and dynamic seepage pressure downslope, which accelerates the movements along the slip surfaces in bedrock. The groundwater level fluctuations are helpful to understand why the deformation response of the middle and

upper parts of the landslide lagged behind the reservoir drawdown.

Deformation characteristics of the Majiagou landslide with piles

Failure mode of the Majiagou landslide

Based on the field investigations and monitoring results, the locations of three slip surfaces S1, S2, and S3 were confirmed (Fig. 12). The failure mode of the Majiagou landslide is controlled by the weak layers in the bedrock and the reservoir level. The date of initiation of the movement along these slip surfaces can be estimated from the timing of the reservoir impoundment and the

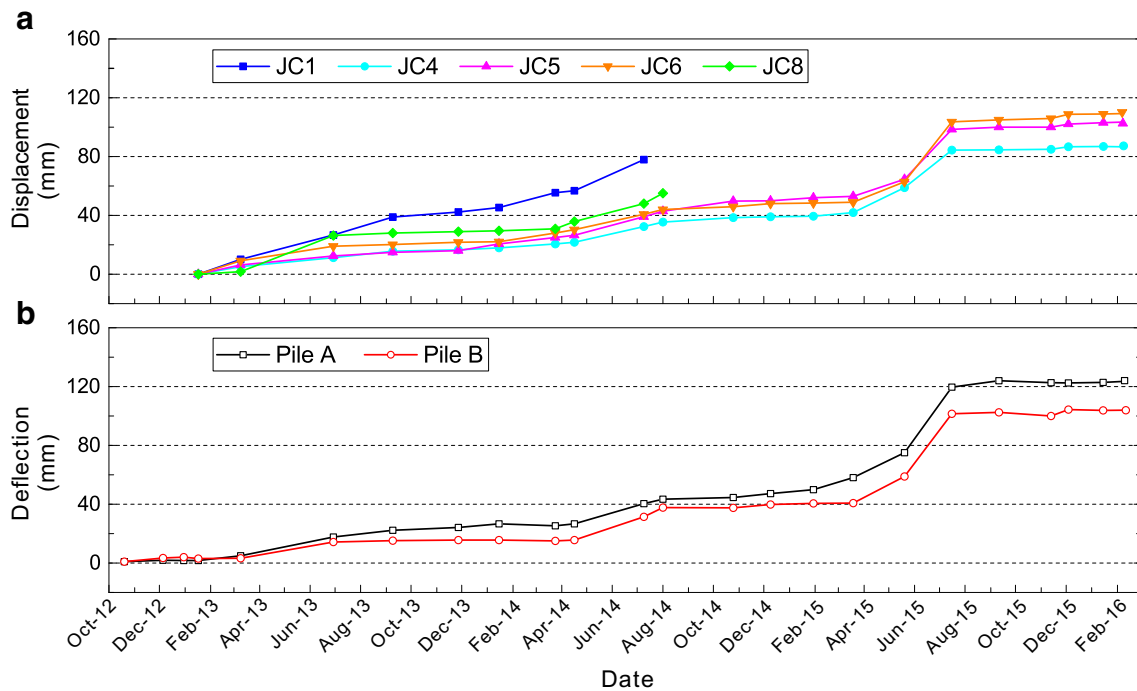


Fig. 10 Time-series of a displacement at the top of inclinometers and b deflection at the top of piles

appearance of surface cracks (Fig. 13). The sequence of events is listed below.

1. In June 2003, the reservoir was first impounded to 135 m (below S₁). The lower part of S₃ was immersed and softened in the groundwater. After 3 months, crack C₁ appeared, coinciding with the initiation of the slip surface S₃.
2. In March 2005, slip surface S₁ was found by geological drilling (25 m length) and shaft excavation (15 m depth). No deeper slip surfaces and groundwater were found between the surface and a depth of 25 m.
3. In October 2006, the reservoir was first impounded to 156 m.
4. In January 2007, a row of 17 anti-sliding piles was installed to treat the slip surface S₁. The other slip surfaces and groundwater were not found in the pile holes.
5. In November 2008, the reservoir was first impounded to 169 m. The front part of S₂ which passes through the bottom of the row of piles was immersed and softened in groundwater.
6. In June 2009, crack C₃ appeared at the end of the reservoir drawdown. The lower part of slip surface S₂ was initiated.
7. In July 2010, crack C₂ appeared, and crack C₃ enlarged after the reservoir was drawn down. These indicate that the slip surface S₂ extended upslope to the ground surface.

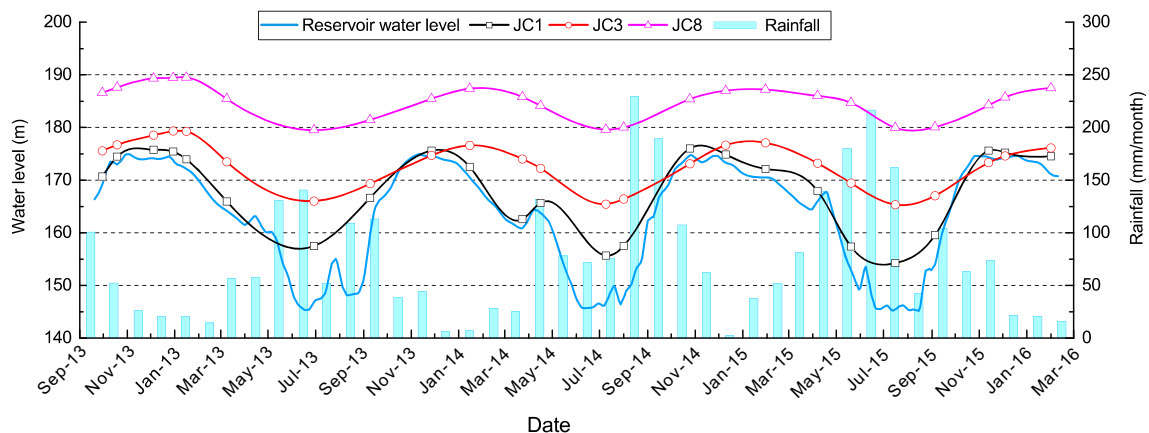


Fig. 11 Time-series of groundwater levels

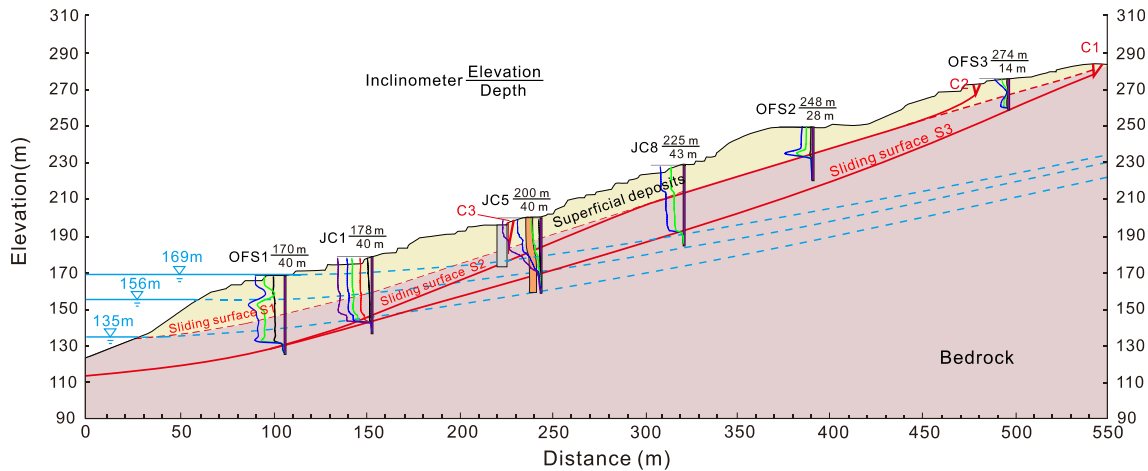


Fig. 12 Deformation and failure mode of Majiagou landslide-stabilizing piles system

From this history, the dates of initiation of shear displacements on S3 and S2 were determined. However, there is no evidence to estimate when slip along S1 initiated, and it is difficult to determine the effectiveness of the row of anti-slide piles for stopping movements along this slip surface.

When the reservoir is drawn down, the lag in the drop in the groundwater level in the bedrock increases the dynamic water pressure and accelerates the landslide motion along the slip surfaces S3 and S2. The rainfall infiltration may increase the weight of superficial deposits and soften the slip surface S1. However, now that the landslide is moving along slip surfaces S3 and S2, the slip surface S1 is relatively stable. This indicates that the reservoir drawdown has a more important influence on the deformation of the Majiagou landslide than rainfall.

Deformation characteristics of landslide with piles

The original row of piles was never able to stabilize the full depth of the landslide because they were too short, and they were sliding with the lower portion of the landslide along slip surface S2. The test piles were long enough to penetrate into the stable bedrock beneath slip surface S3 and thus provided some resistance for the

upslope portion of the landslide and reduced its deformation response to reservoir drawdown and rainfall. However, the portion of the landslide downslope of the piles was still affected by reservoir drawdown.

The two test piles are not sufficient to stabilize the overall landslide motion although they may have reduced movements for a time. After another cycle of reservoir drawdown and rainfall, the landslide movement and pile bending increased and the anti-slide effect of the piles decreased. The deformation characteristics of the portion of the landslide upslope from the piles gradually reverted back to seasonal stepwise cumulative displacements.

Discussion

The reservoir level and rainfall combined to create a yearly seasonal period of accelerated landslide movement. The peak rates of landslide movement do not occur when the reservoir elevation is highest. Instead, they occur 2 to 3 months after reservoir drawdown begins. This period also typically corresponds to the rainy season at the site. In order to determine the domain factor, the velocity of Go1, and the monthly reservoir water level drawdown (2 months ago), and the rainfall

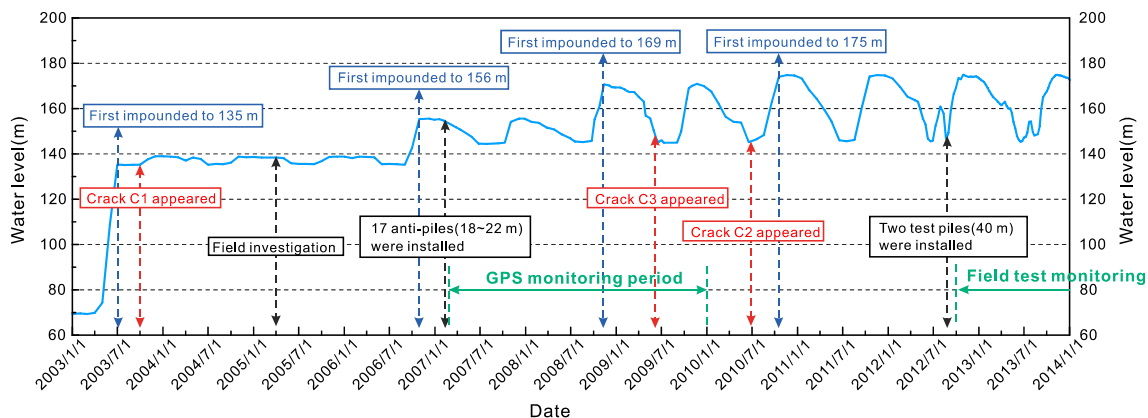


Fig. 13 Time-series of reservoir impoundments, appearances of cracks, and engineering measures

intensity measured from the year 2007 to 2009 were selected as calculation sequences. Based on the Grey relational analysis approach (Deng 1989), the correlation between the G_{01} velocity and water level drawdown is 0.835 and the correlation between the G_{01} velocity and rainfall is 0.727. This indicates that reservoir drawdown is the dominant factor with respect to rainfall. However, the changes in the reservoir level and the rainfall have different effects on different sliding layers of the landslide. Moreover, before and after the test piles were installed, the deformation responses are different too. In this paper, the different deformation responses of the different parts of the landslide are described. In a future research paper, the quantitative relationships between reservoir level, rainfall, and deformation of three sliding layers will be studied by data mining and more in-depth analysis.

Monitoring results show that the GPS displacements for the ground surface are greater than the cumulative inclinometer measurements at the same place. This issue has been found in the field monitoring data of other landslides such as the Huangtupo landslide (Sun et al. 2016) and the Baijiabao landslide (Lu et al. 2016). The first reason may be a loss in measuring range and accuracy due to a distorted installation of the inclinometers. The second reason may be that there are deeper slip surfaces below the known surfaces. For these reasons, the GPS displacements probably capture the real movement of the landslide. To determine if there are any deeper slip surfaces below S_3 at the Majiagou landslide, longer inclinometers will be installed in the near future.

Conclusions

The Majiagou landslide was found to experience movements along three different slip surfaces. The deepest slip surface is the main sliding surface, and it was initiated by the first impoundment in 2003. An intermediate-depth slip surface was initiated by the reservoir drawdown in 2009. The shallowest slip surface was found to be relatively stable under current conditions with the piles installed.

The deformations of the Majiagou landslide respond to the reservoir drawdown and rainfall. There is a 2- to 3-months lag between the reservoir drawdown and the highest movement rates. This is likely caused by the low permeability of the bedrock which delays the drop in the groundwater level. The lag time of the groundwater drops corresponds to the lag time of the landslide deformation response to reservoir drawdown.

The portion of the landslide downslope of the test piles is still affected by the reservoir even with piles. The displacement of the portion of the landslide upslope of the test piles was partially resisted by the test piles. However, as the landslide continued to move and the piles bent, the anti-slide effect of the piles decreased. The test pile deflections were caused by the differential movement along the three slip surfaces of the landslide. The deformation of the landslide-stabilizing pile system reverted to seasonal stepwise cumulative displacements.

The effect of reservoir drawdown and rainfall creates dynamic loads on the landslide-stabilizing pile system. Landslide movement can be triggered by the cycles of reservoir drawdown and rainfall if the sliding resistance provided by the piles is not enough, although the landslide can be slowed down for a time.

Acknowledgements

This study was supported by the Key National Natural Science Foundation of China (41630643), the National Natural Science Foundation of China (41272305), the National Basic Research Program of China (973 Program, No. 2011CB710604).

References

- Chen CY, Martin GR (2002) Soil–structure interaction for landslide stabilizing piles. *Comput Geotech* 29(5):363–386. [https://doi.org/10.1016/S0266-352X\(01\)00035-0](https://doi.org/10.1016/S0266-352X(01)00035-0)
- Cojean R, Cai YJ (2011) Analysis and modeling of slope stability in the Three-Gorges Dam reservoir (China)—the case of Huangtupo landslide. *J Mt Sci* 8(2):166–175. <https://doi.org/10.1007/s11629-011-2100-0>
- Deng J (1989) Introduction to Grey system theory. *J Grey Syst* 1(1):1–24
- Frank R, Pouget P (2008) Experimental pile subjected to long duration thrusts owing to a moving slope. *Géotechnique* 58(8):645–658. <https://doi.org/10.1680/geot.2008.58.8.645>
- Guo WD (2015) Nonlinear response of laterally loaded rigid piles in sliding soil. *Can Geotech J* 52(7):903–925. <https://doi.org/10.1139/cgj-2014-0168>
- He KQ, Li XR, Yan XQ, Guo D (2008) The landslides in the Three Gorges Reservoir region, China and the effects of water storage and rain on their stability. *Environ Geol* 55(1):55–63. <https://doi.org/10.1007/s00254-007-0964-7>
- Hu XL, Zhang M, Sun MJ, Huang KX, Song YJ (2013) Deformation characteristics and failure mode of the Zhujiadian landslide in the Three Gorges Reservoir, China. *Bull Eng Geol Environ* 74(1):1–12. <https://doi.org/10.1007/s10064-013-0552-x>
- Jia GW, Zhan LT, Chen YM, Fredlund DG (2009) Performance of a large-scale slope model subjected to rising and lowering water levels. *Eng Geol* 106(1–2):92–103. <https://doi.org/10.1016/j.enggeo.2009.03.003>
- Jian WX, Wang ZJ, Yin KL (2009) Mechanism of the Anleshi landslide in the Three Gorges Reservoir, China. *Eng Geol* 108(1–2):86–95. <https://doi.org/10.1016/j.enggeo.2009.06.017>
- Jiang QH, Zhou CB (2017). A rigorous solution for the stability of polyhedral rock blocks. *Comput Geotech* 90:190–201. <https://doi.org/10.1016/j.compgeo.2017.06.012>
- Jiang QH, Wei W, Xie N, Zhou CB (2016) Stability analysis and treatment of a reservoir landslide under impounding conditions: a case study. *Environ Earth Sci* 75(1):2. <https://doi.org/10.1007/s12665-015-4790-z>
- Jiao YY, Zhang HQ, Tang HM, Zhang XL, Adoko AC, Tian HN (2014) Simulating the process of reservoir-impoundment-induced landslide using the extended DDA method. *Eng Geol* 182:37–48. <https://doi.org/10.1016/j.enggeo.2014.08.016>
- Kourkoulis R, Gelagoti F, Anastasopoulos I, Gazetas G (2011) Hybrid method for analysis and design of slope stabilizing piles. *J Geotech Geoenviron* 138(1):1–14. [https://doi.org/10.1061/\(ASCE\)GT.1943-5606.0000546](https://doi.org/10.1061/(ASCE)GT.1943-5606.0000546)
- Lane PA, Griffiths DV (2000) Assessment of stability of slopes under drawdown conditions. *J Geotech Geoenviron* 126(5):443–450. [https://doi.org/10.1061/\(ASCE\)1090-0241\(2000\)126:5\(443\)](https://doi.org/10.1061/(ASCE)1090-0241(2000)126:5(443))
- Lirer S (2012) Landslide stabilizing piles: experimental evidences and numerical interpretation. *Eng Geol* 149–150(s 149–150):70–77. <https://doi.org/10.1016/j.enggeo.2012.08.002>
- Li CD, Wu JJ, Tang HM, Hu XL, Liu XW et al (2016) Model testing of the response of stabilizing piles in landslides with upper hard and lower weak bedrock. *Eng Geol* 204:65–76. <https://doi.org/10.1016/j.enggeo.2016.02.002>
- Lu SQ, Zhang GD, Yi QL, Yi W, Huang HF (2016) Characteristics and mechanism of dynamic deformation of baijiabao landslide with stepwise in three gorges reservoir area. *South-to-North Water Transfers Water Sci Technol* 14(3):144–149 (in Chinese). <https://doi.org/10.13476/j.cnki.nsbdqk.2016.03.025>
- Ma JW, Tang HM, Hu XL, Bobet A, Zhang M, Zhu TW et al (2017) Identification of causal factors for the Majiagou landslide using modern data mining methods. *Landslides* 14(1):311–322. <https://doi.org/10.1007/s10346-016-0693-7>
- Massey CI, Petley DN, McSaveney MJ (2013) Patterns of movement in reactivated landslides. *Eng Geol* 159:1–19. <https://doi.org/10.1016/j.enggeo.2013.03.011>
- Palis E, Lebourg T, Tric E, Malet JP, Vidal M (2017) Long-term monitoring of a large deep-seated landslide (La Clapière, south-east French Alps): initial study. *Landslides* 14(1):155–170. <https://doi.org/10.1007/s10346-016-0705-7>
- Paronuzzi P, Rigo E, Bolla A (2013) Influence of filling–drawdown cycles of the Vajont reservoir on Mt. Toc slope stability. *Geomorphology* 191(1):75–93. <https://doi.org/10.1016/j.geomorph.2013.03.004>

- Sharafi H, Sojoudi Y (2016) Experimental and numerical study of pile-stabilized slopes under surface load conditions. *Int J Civil Eng* 14(4):221–232. <https://doi.org/10.1007/s40999-016-0017-2>
- Smethurst JA, Powrie W (2007) Monitoring and analysis of the bending behaviour of discrete piles used to stabilise a railway embankment. *Géotechnique* 57(8):663–677. <https://doi.org/10.1680/geot.2007.57.8.663>
- Sun GH, Zheng H, Tang HM, Dai FC (2016) Huangtupo landslide stability under water level fluctuations of the three gorges reservoir. *Landslides* 13(5):1167–1179. <https://doi.org/10.1007/s10346-015-0637-7>
- Sun YJ (2015) Bank slope multi-fields monitoring based on fiber optic sensing technologies and stability evaluation study. Dissertation, Nanjing University
- Wang FW, Zhang YM, Huo ZT, Peng XM, Araiba K, Wang GH (2008) Movement of the Shuping landslide in the first four years after the initial impoundment of the Three Gorges Dam Reservoir, China. *Landslides* 5(3):321–329. <https://doi.org/10.1007/s10346-008-0128-1>
- Wang JE, Su AJ, Xiang W, Yeh HF, Xiong CR, Zou ZX et al (2016) New data and interpretations of the shallow and deep deformation of Huangtupo no. 1 riverside sliding mass during seasonal rainfall and water level fluctuation. *Landslides* 13(4):795–804. <https://doi.org/10.1007/s10346-016-0712-8>
- Wei WB, Cheng YM, Li L (2009) Three-dimensional slope failure analysis by the strength reduction and limit equilibrium methods. *Comput Geotech* 36(1–2):70–80. <https://doi.org/10.1016/j.compgeo.2008.03.003>
- Xia M, Ren GM, Ma XL (2013) Deformation and mechanism of landslide influenced by the effects of reservoir water and rainfall, Three Gorges, China. *Nat Hazards* 68(2):467–482. <https://doi.org/10.1007/s11069-013-0634-x>
- Yan ZL, Wang JJ, Chai HJ (2010) Influence of water level fluctuation on phreatic line in silty soil model slope. *Eng Geol* 113(1):90–98. <https://doi.org/10.1016/j.enggeo.2010.02.004>
- Yin YP, Wang HD, Gao YL, Li XC (2010) Real-time monitoring and early warning of landslides at relocated Wushan town, the Three Gorges Reservoir, China. *Landslides* 7(3):389–389. <https://doi.org/10.1007/s10346-010-0220-1>
- Yi W, Meng ZP, Yi QL (2011) Theory and method of landslide stability prediction in the Three Gorges Reservoir area. Science Press, Beijing
- Zhou CM, Shao W, Westen CJV (2014) Comparing two methods to estimate lateral force acting on stabilizing piles for a landslide in the Three Gorges Reservoir, China. *Eng Geol* 173(6):41–53. <https://doi.org/10.1016/j.enggeo.2014.02.004>
- Zhu HH, Shi B, Yan JF, Zhang J, Zhang CC, Wang B (2014) Fiber Bragg grating-based performance monitoring of a slope model subjected to seepage. *Smart Mater Struct* 23(9):639–650. <https://doi.org/10.1088/0964-1726/23/9/095027>

Y. Zhang · X. Hu (✉) · G. Zhang · F. Tan

Faculty of Engineering,
China University of Geosciences,
Wuhan, Hubei 430074, People's Republic of China
Email: huxinli@cug.edu.cn

D. D. Tannant

School of Engineering,
University of British Columbia,
Kelowna, BC V1V 1V7, Canada